***Розглядається зміна енергії Гіббса у момент виникнення пори. Виводяться умови існування пори, час виникнення пори і знайдена ймовірність виникнення пори. Також наводяться експериментальні дослідження швидкості пороутворення і швидкості росту пор глиноземистих матеріалів. Отримані результати застосовні для таких теплоізоляційних матеріалів, як керамзит і вогнетриви, а також інших матеріалів на основі глинозему***

***Ключові слова: пори, пориста система, швидкість пороутворення, енергія Гіббса, глинозем, керамзит, вогнетриви***

***Рассматривается изменение энергии Гиббса в момент возникновения поры. Выводятся условия существования поры, время возникновения поры и найдена вероятность возникновения поры. Также приводятся экспериментальные исследования скорости порообразования и скорости роста пор глиноземистых материалов. Полученные результаты применимы для таких теплоизоляционных материалов, как керамзит и огнеупоры, а также прочих материалов, на основне глинозему***

***Ключевые слова: поры, пористая система, скорость порообразования, энергия Гиббса, глинозем, керамзит, огнеупоры***

УДК 53.09, 536.4.033, 536.416, 66.040.262
DOI: 10.15587/1729-4061.2016.66033

# A STUDY OF THE RATES OF PORE NUCLEATION AND PORE GROWTH IN ALUMINA-BASED THERMAL INSULATION MATERIALS

**A. Cheilytko**
Candidate of technical sciences,
Associate Professor
Doctoral student at the department
of thermal power engineering
Zaporizhzhya state engineering academy,
Lenina ave., 226, Zaporizhzhya, 69006, Ukraine
E-mail: cheylitko@yandex.ua

## 1. Introduction

Research on energy processes in porous materials is a separate course in thermal physics and thermal power engineering, as their structure facilitates rather complex heat and mass transfer processes, which have been insufficiently studied. The existing theories for individual cases and semi-empirical dependencies do not cover the entire area and the whole variety of porous materials.

Thermal insulation is the most interesting property of the entire set of the porous materials is the power industry. Thermal characteristics of thermal insulation determine efficiency of energy-saving measures and technologies. Among the variety of thermal insulation materials, the medium and high-temperature insulation types that are used both in construction and metallurgical production are alumina-based materials and silicates. The porosity of these materials largely affects their thermophysical characteristics [1, 2]. However, porosity is a whole set of parameters rather than a single value. If the total porosity is the same, but the amounts of pores are different, the thermal conductivity properties of such materials are different [3].

The importance of the study is determined by its attention to the kinetics of changes in porosity, which makes it possible to create a basis for developing new high-intensity technologies in various industries, particularly to improve the production technology of thermal insulation materials based on alumina.

## 2. Analysis of previous studies and statement of the problem

There are both different approaches to porosity and various classifications of pores [3, 4]. However, to obtain the necessary thermal properties of a material, it is important to be able to predict changes in both the porosity and the number of pores. For example, study [3] describes an equation that allows analytical counting of pore nucleation sites at a certain time. However, this equation includes the energy of activating pore nucleation sites, which can only be determined by kinetic experiments. The method of kinetic experimentation to determine the activation energy of pores development is not described in the study.

In [5], a description of a porous structure is provided to allow mathematical specification of the thermophysical processes occurring in the material. However, the author does not consider the possibility of controlling the porous structure.

Study [6] analyzes the porous structure of silicon carbide (SiC) in ceramics. It reveals the basic reactions in obtaining silicon carbide and dependence of the ceramic product porosity on the synthesis of the initial components. In [6], pictures are provided to illustrate the obtained material structure and its porosity, but even with the same porosity the observed structures are completely different. The study also shows dependence of thermal conductivity on porosity. Among the porous structure parameters, only location uniformity and pores shapes are considered alongside the total porosity.

In [7], the authors consider a mathematical model of a vapor bubble growth in an unrestricted space. Theoretically, this model can be used for clay aggregate expansion with water vapor. However, there is no experimental evidence of this.

In [8], clay aggregate concretes of different pore structures are obtained by varying the composition of the initial mixture and the heat treatment temperature. In [9], lightweight expanded clay aggregate (LECA) is exposed to heat according to the standard ISO-834 temperature curve, and the resulting structure is consequently studied. However,



© A. Cheilytko, 2016

the authors do not develop a clear pattern of how the temperature and the composition of the initial mixture affect the resulting porous structure.

In [10], a mathematical description is suggested for considering a porous structure in a three-dimensional space. The author examines diffusion and microconvection currents in the porous material. The suggested method does not account for any pore size or pore shape. Moreover, the author does not consider any way of creating such a porous structure.

In [11], research is described on the influence of pressure in pores on elastomers of closed porosity. Pressure changes in pores are considered under different hydrostatic loads, with a conclusion that pressure can significantly change the macroscopic reaction and stability of closed porosity elastomers. However, the study does no suggest a method of calculating pressure in pores, and the initial pressure is just taken as ambient pressure. It is also assumed in the study that pressure in pores is only a density function.

In [12], changes in a closed porosity structure are studied under compression and expansion at different initial pressures in pores. The experimental results show that pressure in pores has a positive effect in the case of compression and an adverse effect in the case of stretching. However, the study does not consider any method of achieving those or other pressures in the pores of the material or any method of their calculation.

In [13], porosity is shown to have a positive effect even on metal alloys, but no method is provided to manage porosity.

The analysis of the previous studies results in a conclusion that it has not been yet determined how to calculate the rates of pore nucleation and pore growth in intumescent materials. Besides, there has not been any mathematical solution suggested for calculating thermodynamic parameters of the state of gas inside closed pores. These problems make it impossible to control the thermal properties of alumina-based material during its formation.

## 3. The purpose and objectives of the study

The purpose is to study the rates of pore nucleation and pore growth in alumina-based thermal insulation materials.

To achieve this purpose, the following objectives have been formulated:

– to find the conditions in which pores can exist;

– to determine analytically the time when a pore appears;

– to identify common dependencies in the changing number of pores and porosity when swelling alumina-based materials;

– to develop a mathematical model that describes changes in the number of pores in an alumina-based material.

## 4. The critical radius of a spherical pore nucleus and pore growth conditions

The Gibbs energy of the material-pore system during pore formation will change for the value of $\Delta G$. This value will comprise two parts, the first of which is equal to the result of the difference between the chemical potential of the new gas and the original gas multiplied by the resulting constitutive pore nucleating agent. The other element of the equation is determined by the surface energy:

$$\Delta G = \left(\varphi^{(1)} - \varphi^{(pre)}\right) \cdot M^{(1)} + \sigma\Omega,$$

where $\Delta G$ is the mass of the pore nucleating agent; $\Omega$ – is the outside surface of the pore nucleating agent; $\varphi^{(1)}$ – is the chemical potential of the pore nucleating gas; index (1) refers to the gas pore; index (pre) refers to the pore nucleating agent.

For a spherical particle:

$$\Delta M^{(1)} = \frac{4}{3}\frac{\pi}{\upsilon'} r^3;\ \Omega = 4\pi r^2.$$

Therefore:

$$\Delta G = \frac{4\pi}{3}\left(\varphi^{(1)} - \varphi^{(pre)}\right)\frac{r^3}{v^{(1)}} + 4\pi\sigma r^2. \quad (1)$$

The equation of the Gibbs energy change is differentiated by the radius and equated to zero:

$$\left(\varphi_\infty^{(1)} - \varphi_\infty^{(pre)}\right)\frac{\left(r_{kr}^{(1)}\right)^2}{v^{(1)}} + 2\sigma r_{kr}^{(1)} = 0.$$

In the given equation, the values of the chemical potentials of substances are accepted for an infinite radius (with a linear interface) so that they could be beyond the sign of differentiation.

The critical radius will be equal to the following:

$$r_{kr}^{(1)} = \frac{2\sigma\upsilon^{(1)}}{\varphi_\infty^{(pre)} - \varphi_\infty^{(1)}},$$

where $\varphi_\infty^{(pre)}$ is a chemical potential of the raw material of the pore nucleating agent; $\varphi_\infty^{(1)}$ is a chemical potential of the pore nucleating agent outside the pore.

If in the raw material there appears a pore nucleus with a diameter of $r_{кр}^{(1)}$, it will be in equilibrium with its surrounding material. The pressure of the pore nucleating agent will be lower than the pressure of the same gas in the natural environment and lower than the pressure of the surrounding material [2]. This means that the equilibrium state is metastable. Without any external energy supply to the pore or a reduced stress tensor, the pore nucleus will disappear – it will be absorbed by the material.

At $r^{(1)} > r_{kr}^{(1)}$, there are several development options.

In the first option, if $\varphi^{(1)} - \varphi^{(pre)} < 0$ and the r is small, the second element of the expression (1) will prevail. As the r develops, the $\Delta G$ will increase, which means that creation of a tiny pore nucleus will increase the Gibbs energy. The $\Delta G$ will be increasing until the first and the second members of the expression for $\partial G / \partial r$ become equal, i. e. until the r reaches the value of $r = r_{kr}^{(1)}$, which maximizes the Gibbs energy; if the value corresponds to the expression $r > r_{kr}^{(1)}$, the energy decreases. The aforementioned is shown schematically in Fig. 1.

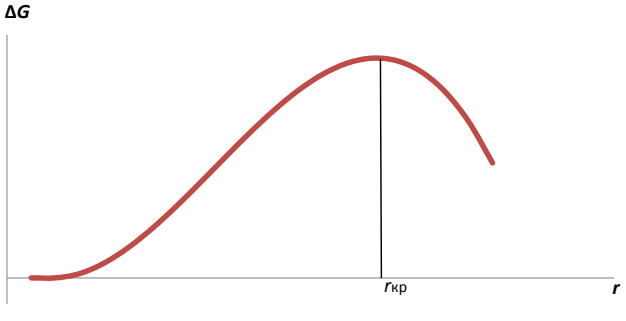


Fig. 1. Changes in the Gibbs energy $\Delta G$ with the radius r at $\varphi^{(1)} - \varphi^{(pre)} < 0$ and with a small radius

The second possibility occurs if $\varphi^{(1)}-\varphi^{(pre)}>0;$ then at any value of the radius r the Gibbs energy increases, and the system is trying to absorb the pore.

In any case, if the original size of the pore nucleus is less than $r_{кр}^{(1)}$, such a nucleus cannot exist for long – it will be downsized until its complete disappearance.

For a pore to exist, the following condition is necessary: $\varphi^{(1)}-\varphi^{(pre)}<0$ In this case, the critical radius is directly proportional to the surface tension ratio. That is, a pore in the initial mixture is more likely to appear in areas with low surface tension (such an area can be generated by density fluctuations).

## 5. The work of pore creation and the time of pore nucleation

The work of the reversible formation of a spherical pore nucleus $l'^{(1)}_{min}$ at T=const and V=const is represented by the following:

$$l'^{(1)}_{min}=-\left(p^{(1)}-p\right)\frac{4}{3}\pi r^{(1)3}+4\pi r^{(1)2}\sigma.$$

Before the pore nucleation, the volume of the initial phase was equal to $V+V^{(1)}$ $\left(V^{(1)}=\frac{4}{3}\pi r^{(1)3}\right)$, with the pressure p; after the nucleus formation, the volume remained the same, but the pressure in the pore nucleus surrounding area became equal to $p^{(1)}$, i. e. it had decreased by $p-p^{(1)}$. The respective work done was $-\int V^{(1)}dp=-\left(p^{(1)}-p\right)\frac{4}{3}\pi r^{(j)3}$; besides, the expression $l'^{(1)}_{min}$ started to include the surface energy $4\pi r^{(1)2}\sigma$,

As according to [2]

$$p^{(1)}-p=\frac{2\sigma}{r^{(1)}},$$

the expression for $l'^{(1)}_{min}$ is the following:

$$l^{,(1)}_{min}=\frac{4}{3}\pi\sigma r^{(1)2}.$$

As seen from the equation, the work of a pore nucleation and the work of the pore growth are different.

The work of creating a pore nucleus of a critical size will be as follows:

$$l^{(1)}_{kr}=\frac{16}{3}\pi\sigma^2\frac{\upsilon^{(1)}}{\varphi^{(pre)}_{\infty}-\varphi^{(1)}_{\infty}},$$

or, taking into account that $r^{(1)}=\frac{2\sigma}{p^{(1)}-p}$, the equation is the following:

$$l^{(1)}_{kr}=\frac{16}{3}\pi\frac{\sigma^3}{\left(p^{(1)}_{kr}-p\right)^2}.$$

The frequency of forming a spontaneous nucleus can be represented as in [2]:

$$J=N_1\cdot B\cdot e^{-\frac{l^{(1)}_{kr}}{k_B\cdot T}},$$

where $N_1$ is the number of molecules of the pore nucleating agent per unit volume; B is a kinetic factor, non-defined by the authors; $\frac{l^{(1)}_{kr}}{k_B\cdot T}$ is the relative height of the free-energy barrier for nucleation; this term of the equation can be considered as a parameter of the nucleation stability of the material.

The pore nucleus detection time can be represented by the following:

$$\tau_s=\overline{\tau}_з+\tau_p,$$

where $\tau_s$ is the observation time; $\overline{\tau}_з$ is the average time of expecting a pore nucleus to appear; $\tau_p$ is the system relaxation time determined by the pores genesis.

As the frequency of pore nuclei formation is the number of nuclei that emerge during an observed unit of time, then:

$$\overline{\tau}_з=\frac{n_{пор}}{N_1\cdot B\cdot e^{-\frac{l^{(1)}_{кр}}{k_B\cdot T}}}-\tau_p. \quad (2)$$

In this equation, the only unknown parameter is the kinetic factor B that has to be found empirically.

## 6. Probability for a pore to develop from a nucleus of a critical radius

Let us introduce a probability parameter P for a pore to develop from a nucleus; the P will be understood as the number of pores k per unit time related to the number of the nuclei $n_{pore}$:

$$p=\frac{k}{\Delta\tau\cdot n_{pore}}.$$

According to the binominal distribution, the probability that the k of nuclei will become pores is described by the equation:

$$P(k)=C^k_n\cdot p^k\cdot(1-p)^{n-k},$$

where $C^k_n$ is a binominal coefficient:

$$C^k_n=\frac{n!}{k!(n-k)!}.$$

Let us introduce the notation $p\cdot n=w$ as an expected value. This is the sequence of pores emergence over time, which constitutes a flow of pore formation. The physical meaning is the probability density of pore nucleation, i. e. the ratio limit value of the probability that at least one pore will appear within the time interval expressed as follows:

$$w(\tau)=\lim_{\Delta\tau\to 0}\frac{P(\tau,\tau+\Delta\tau)}{\Delta\tau}.$$

The probability that a nucleus of the critical radius will be self-destroyed is q=1–p.

As it is necessary to achieve the most favourable conditions for a nucleus to develop into a pore, self-destruction of the nucleus complies with the requirements of the Poisson distribution, which determines the following:

$$Q(k)=\frac{w_0^{\,k}}{k!}e^{-w_0},$$

where $w_0$ is the expected value the nucleus self-destruction $w_0=q\cdot n$.

According to the Poisson distribution, $w_0=\text{const}$. For these conditions, the probability of k pores to be created out of n nuclei of the critical radius will be equal to the following:

$$P(k)=1-\frac{w_0^{\,k}}{k!}e^{-w_0}.$$

Thus, formation of at least one pore within the time τ will be equal to the following:

$$\int_{Q(0)}^{Q(\tau)} \frac{dQ(\tau)}{Q(\tau)} = \int_{0}^{\tau} -w_0 d\tau,$$

$$\ln Q(\tau) = -w_0 \tau,$$

$$Q(\tau) = e^{-w_0 \tau},$$

or

$$P(\tau) = 1 - e^{-\omega_0 \tau}.$$

These equations make it possible to predict a probability that the necessary amount of pores can appear according to statistical data (a pore nucleation matrix). In other words, porosity of a material can be predicted (with a certain error) on the basis of pore-formation observations in a particular material.

## 7. The results and analysis of the experiment to determine the porosity and the number of pores in an intumescent alumina-based material

The experiment was carried out in the following way. An initial wet mixture was placed into numerated dry ceramic containers and subjected to heat treatment in a muffle furnace at different temperatures to determine the activation energy of pore formation by the resulting gases. The selected temperatures were 120 °C and 200 °C. Two samples were alumina-based. Both samples were saturated with moisture up to about 30 %. The first sample was based on a mixture of chamotte and clay, and the second was a mixture of clay, chamotte, and a plasticizer. Each sample was dried at room temperature (without swelling the sample); its porosity and volume were considered as initial values. Then samples were taken out of each sample from the furnace at 3, 5, 10, 15 and 20 minutes after the start of the heat treatment. The constant of the pore nucleation speed and the constant of porosity growth were determined for each moment of time, with further calculation of their average value. The number of pores was considered on the area of 9 mm$^2$.

Tables 1, 2 show the experiment results. The amount of evaporated moisture was determined by an indirect method.

According to the results of the experiment (Table 1 and Table 2), dependencies were built to determine the patterns of porosity growth and the changes in the number of pores in the alumina-based materials.

Fig. 2 displays wetness dependence of the two samples on the time of heat treatment (at temperatures of 200 °C and 100 °C). Zero wetness was understood as an air-dry state. The dependencies show that the curve of wetness changes in the pore nucleating samples corresponds to the standard curve of wetness changes in drying. Besides, the first part of the curve – a section of constant wetness – is not expressed because of its smallness, which can be explained by too high temperatures in comparison with drying.

Since the dependence of changes in wetness during swelling coincides with the change in wetness during drying, it is interesting to analyse the drying rate curve. Fig. 3 displays the drying rate of the samples at 120 °C and 200 °C. Due to the large time step, it is difficult to single out specific periods of the drying speed. At a temperature of 120 °C, it is conditionally possible to distinguish between periods of increasing, constant and decreasing rates of desiccation, but at 200 °C the rate of desiccation increases too sharply. Fig. 3 reflects how the rate of desiccation changes and, consequently, (with account for the time delay) how pores are formed in the material. This dependence between the process of desiccation and the porosity changes is highly interesting from a scientific point of view.

Table 1

The number of pores and the porosity of sample 1 depending on the heat treatment time

| τ, min | t, °C | | | | | |
|---|---|---|---|---|---|---|
| | 120 | | | 200 | | |
| | n, pc/9 mm$^2$ | P/P$_0$, % | W$_{ev}$, % | n, pc/9 mm$^2$ | P/P$_0$, % | W$_{ev}$, % |
| 3 | 13 | 1.05 | 6.98 | 23 | 1.1 | 20.59 |
| 5 | 9 | 1.08 | 15.24 | 21 | 1.12 | 26.72 |
| 10 | 8 | 1.01 | 27.73 | 18 | 1.13 | 27.11 |
| 15 | 7 | 1.011 | 30.01 | 10 | 1.15 | 30.01 |
| 20 | 5 | 1.01 | 30.01 | 9 | 1.17 | 30.01 |

Table 2

The number of pores and the porosity of sample 2 depending on the heat treatment time

| τ, min | t, °C | | | | | |
|---|---|---|---|---|---|---|
| | 120 | | | 200 | | |
| | n, pc/9 mm$^2$ | P/P$_0$, % | W$_{ev}$, % | n, pc/9 mm$^2$ | P/P$_0$, % | W$_{ev}$, % |
| 3 | 8 | 1.01 | 5.23 | 10 | 1.7 | 18.02 |
| 5 | 8 | 1.4 | 12.36 | 9 | 1.95 | 27.12 |
| 10 | 7 | 1.5 | 22.63 | 6 | 2.2 | 28.41 |
| 15 | 5 | 1.6 | 27.6 | 4 | 2.1 | 29.27 |
| 20 | 5 | 1.58 | 29.25 | 4 | 1.5 | 29.27 |

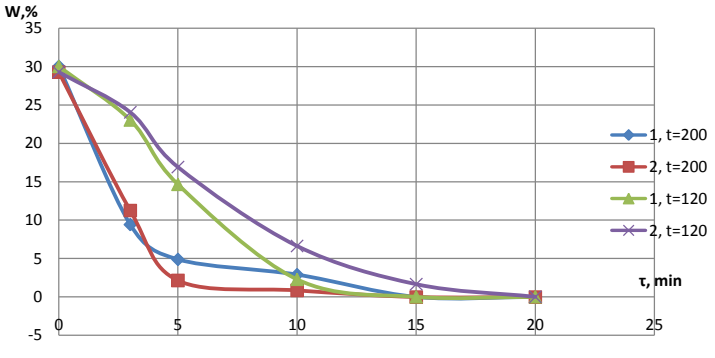


Fig. 2. Changes of wetness W in samples 1 and 2 depending on the time τ of their heat treatment

Fig. 4 shows changes in the number of pores in the samples during the time of the heat treatment. The number of pores was determined by photographing the cross section of a sample, followed by applying a grid and magnifying the selected fragments. The number of pores was counted on an area of 9 mm$^2$ and transferred onto an area of 1 m$^2$ to comply with the dimensions in the system of units (SU). The pores that were taken into account were of the largest geometric size above 0.1 mm. The view of the developed curves is

similar to curves of changes in the wetness of the material. Fig. 4 shows that temperature differently affects the number of pores. In sample 1, the number increased almost 2.5 times, but in a more ductile sample 2 the increase was insignificant and followed by a further reduction.

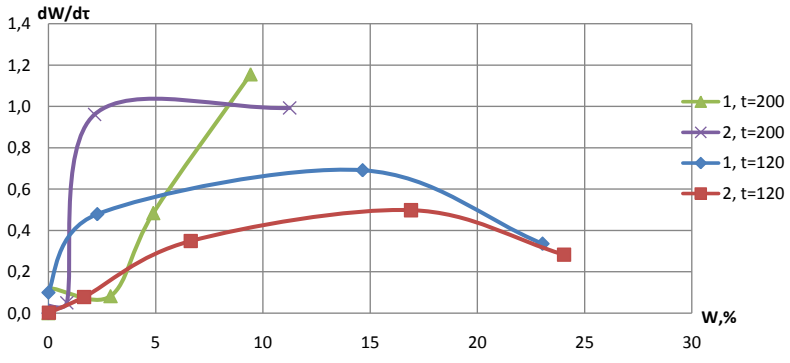


Fig. 3. The speed of drying samples 1 and 2 at different temperatures t

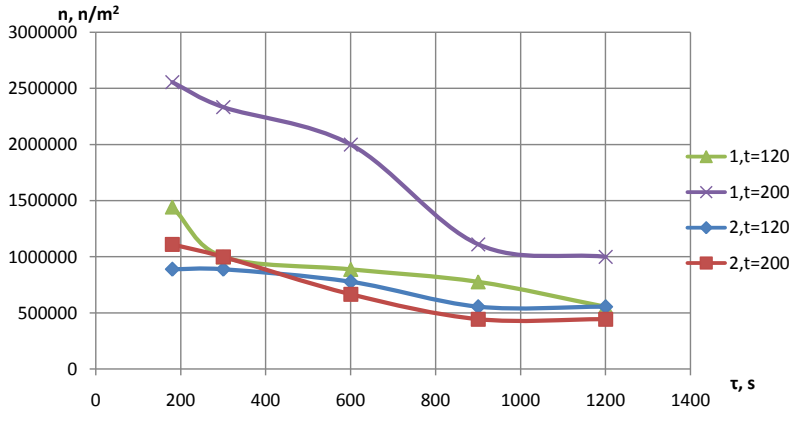


Fig. 4. Changes in the number n of pores in the tested samples throughout the time τ

Judging by (2) it is possible to assume that the number of pores is likely to grow; however, Fig. 4 shows that this is not the case. The reason is that pores grow and merge into a single pore. This shows that for a mathematical analysis of a porous structure it is necessary to solve a system of equations on the increasing number of pores and porosity growth.

In Fig. 4, it is possible to distinguish between three periods of pore formation. The first period depends on the material itself. In the ductile sample 2, the first stage is the stage of a slight decrease in the number of pores. In sample 1, this is the stage of a significant reduction in the number of pores. The second stage coincides with an even (linear) decrease in the number of pores in the material. With an increasing temperature, this dependence becomes steeper, i. e. the number of pores decreases more intensely due to a more intense increase in the pore volume. A comparison of this stage with Fig. 5 shows a reverse relationship with increasing porosity. The third stage is the stage of a further flowing decrease in the number of pores alongside their decreasing or constant volume, i. e. the stage of pores overgrowing. The distinction between the stages allows a more precise predicting of the boundary conditions of the problem.

Changes in the total porosity in the tested samples are shown in Fig. 5, which displays the time dependence of porosity in the samples. A significant increase in porosity can be observed in the ductile sample, which conforms to the previously expressed theory of swelling materials. It is noteworthy that higher temperatures of heat treatment increased the porosity of both samples.

Fig. 6, 7 show dependencies of the pore nucleation rate and the porosity change rate in the samples. For ease of data visualization, in Fig. 6 the rate is referred to with the opposite sign. The pore nucleation rate in the first sample is different from all the others. This is due to the rate of moisture diffusion and the speed the forming the surface crust. Since the temperature and the plasticity of the material are small, water evaporates out of the material before pores are formed. The patterns of the other curves show that the pore formation rate increases at the beginning, but then it slowly fades. The rate of the porosity increase persistently declines, and it is maximal at the initial point – at the time when the liquid vaporizes. Sample 2 in Fig. 7 has a negative pore growth rate – a shrinkage, which is caused by the sample's high plasticity and its long heat treatment.

The completed experiments have identified the main patterns of changes in the number of pores and the total porosity of aluminous materials when they are heat-treated.

The obtained findings can be presented in a resulting model that describes porosity changes in the material:

$$\begin{cases} n_{pore} = \tau_s \cdot N_1 \cdot B \cdot e^{\frac{16\pi\sigma^3}{3k_B \cdot T\left(p_{kr}^{(t)} - p\right)^2}} & \text{if} \quad \tau_s < \tau_1, \\ n_{pore} = \tau_s \cdot \xi_1 \cdot (1-P) & \text{if} \quad \tau_1 < \tau_s < \tau_2, \\ n_{pore} = \tau_s \cdot \xi_2 \cdot P & \text{if} \quad \tau_s > \tau_2, \end{cases}$$

where $\xi_1$ and $\xi_2$ are empirical coefficients.

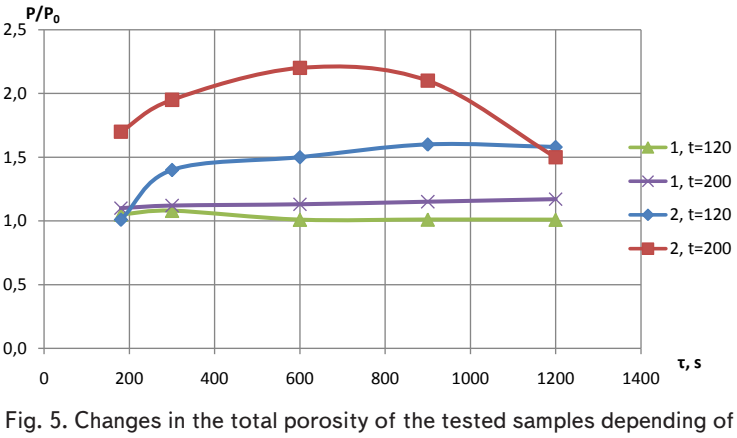


Fig. 5. Changes in the total porosity of the tested samples depending of the heat treatment time τ

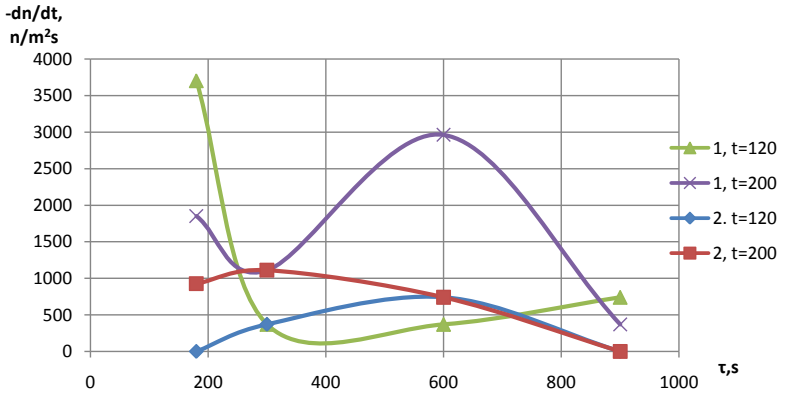


Fig. 6. Changes in the pore nucleation rate in the tested samples depending on the heat treatment time τ

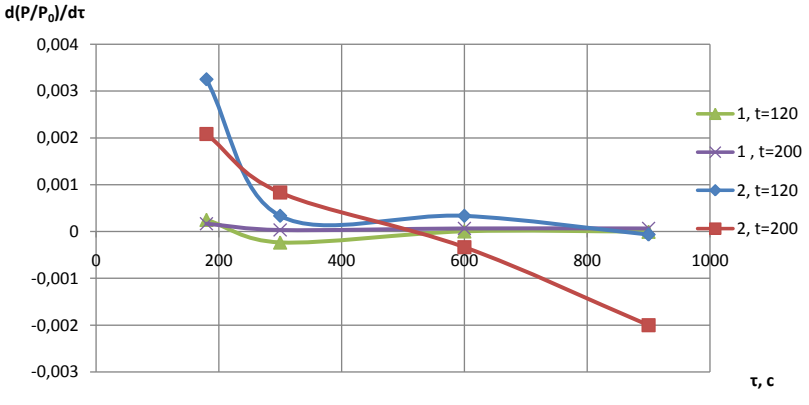


Fig. 7. Dynamics in the samples' porosity depending on the heat treatment time τ

The research findings make it possible to predict the characteristics of the resulting porosity of a material, which can allow controlling the thermal properties of an aluminous material and changing the heat treatment process.

## 8. Conclusion

1. The condition for a pore to exist is $\varphi^{(1)} - \varphi^{(pre)} < 0$ (herewith, a pore in the initial mixture is more likely to occur in a place with a low surface tension).

2. The obtained equation allows calculating the average waiting time for a pore to appear. It is a ratio of the number of pores (from the statistical matrix) to the frequency of a spontaneous nucleation of pores less the relaxation time. This makes it possible to predict the porosity of a material if there is an observation data base about the material. There is also a connection revealed between the number of pores, the critical work of a pore, and time.

3. The undertaken analysis concerned changes in the wetness of porous alumina-based materials, in the amount of pores and in the total porosity while swelling such materials. It has revealed that the curves of the wetness change rate in an intumescent material are similar to the curves of drying, and they also have three periods that respectively reflect increasing, constant and decreasing rates of desiccation. Pores formation can be divided into three periods:

– the first period, which is the stage of a decreasing number of pores, depends on the material (in a more ductile material, the decrease in the number of pores is slight, but if the material if less flexible, the number of pores is reduced substantially);

– the second period is the stage of an equable reduction of the number of pores in the material (an increasing temperature decreases the number of pores more rapidly due to a more intense increase of the pore volume);

– the third period is the stage of pores overgrowing.

4. The study suggests a system of equations that describe changes in the number of pores in an alumina-based material. It allows predicting the number of pores in the swelling of an alumina-based material during its heat treatment. This consequently facilitates control over thermophysical properties of the material.

References

1. Cheylitko, A. A. Study of vesiculation in intumescent material [Text] / A. A. Cheylitko // Technology Audit and Production Reserves. – 2013. – Vol. 5, Issue 4 (13). – P. 38–40. – Available at: http://journals.uran.ua/tarp/article/view/18251/16063
2. Pavlenko, A. M. Gas parameters agent-blowing agent inside a closed spherical pores in a state of equilibrium [Text] / A. M. Pavlenko, H. V. Koshlak, A. A. Cheylitko, M. A. Nosov // Vestnik NTU "KPI", Series: New solutions in modern technologies. – 2015. – Vol. 62, Issue 1171. – P. 28–35.
3. Cheylitko, A. A. Osobennosti vliyaniya poristosti na teploprovodnost glinozemestyih materialovperevoda [Text] / A. A. Cheylitko. – Dnepropetrovsk : Serednyak T. K., 2015. – 76 p.
4. Shpak, A. Klasternye i nanostrukturnye materialy. Vol. 3. Poristost' kak osoboe sostoianie samoorganizovannoi struktury v tverdotel'nyh materialah [Text] / A. Shpak, P. Cheremskoi, Yu. Kunitskii, O. Sobol'. – Kyiv: VD «Akademperiodika», 2005. – 516 p.
5. Freire-Gormaly, M. The Pore Structure of Indiana Limestone and Pink Dolomite for the Modeling of Carbon Dioxide in Geologic Carbonate Rock Formations [Electronic resource] / M. Freire-Gormaly. – University of Toronto, 2013. – Available at: https://tspace.library.utoronto.ca/bitstream/1807/42840/1/Freire-Gormaly_Marina_201311_MASc_thesis.pdf
6. Eom, J.-H. Processing and properties of macroporous silicon carbide ceramics: A review [Text] / J.-H. Eom, Y.-W. Kim, S. Raju // Journal of Asian Ceramic Societies. – 2013. – Vol. 1, Issue 3. – P. 220–242. doi: 10.1016/j.jascer.2013.07.003

7. Pavlenko, A. M. Design of processes of thermal bloating of silicates [Text] / A. M. Pavlenko, H. V. Koshlak // Metallurgical and Mining Industry. – 2015. – Vol. 1. – P. 118–122. – Available at: http://www.metaljournal.com.ua/assets/Journal/english-edition/MMI_2015_1/21%20Pavlenko.pdf
8. Bajare, D. Lightweight Concrete with Aggregates Made by Using Industrial Waste [Text] / D. Bajare, J. Kazjonovs, A. Korjakins // Journal of Sustainable Architecture and Civil Engineering. – 2013. – Vol. 4, Issue 5. doi: 10.5755/j01.sace.4.5.4188
9. Bodnárová L. Behaviour of Lightweight Expanded Clay Aggregate Concrete Exposed to High Temperatures [Text] / L. Bodnárová, R. Hela, M. Hubertová, I. Nováková // International Journal of Civil, Environmental, Structural, Construction and Architectural Engineering. – 2014. – Vol 8, Issue 12. – P. 1205–1208.
10. Dincov, D. D. Heat and mass transfer in two-phase porous materials under intensive microwave heating [Text] / D. D. Dincov, K. A. Parrott, K. A. Pericleous // Journal of Food Engineering. – 2004. – Vol. 65, Issue 3. – P. 403–412. doi: 10.1016/j.jfoodeng.2004.02.011 – Available at: http://www.researchgate.net/publication/222658046
11. Lopez-Pamies, O. Effects of internal pore pressure on closed–cell elastomeric foams [Electronic resource] / O. Lopez-Pamies, P. Ponte Castaneda, M. I. Idiart // International Journal of Solids and Structures. – 2012. – Vol. 49, Issue 19-20. – P. 2793–2798. doi: 10.1016/j.ijsolstr.2012.02.024 – Available at: http://www.researchgate.net/publication/256733990_Effects_of_internal_pore_pressure_on_closed–cell_elastomeric_foams
12. Vesenjak, M. Influence of pore gas in closed–cell cellular structures under dynamic loading [Electronic resource] / M. Vesenjak, A. Öchsner, Z. Ren. – German LS–DYNA Forum. Bamberg, 2005. – Available at: https://www.dynamore.de/de/download/papers/forum04/new–methods/influence–of–pore–gas–in–closed–cell–cellular
13. Komissarchuk, O. Pore structure and mechanical properties of directionally solidified porous aluminum alloys [Electronic resource] / O. Komissarchuk, Z. Xu, H. Hao. – China Foundry. China, 2014. – Available at: https://doaj.org/article/002c72e2e01345db8bf4fef190113057